JOURNAL OF AGRICULTURAL AND FOOD CHEMISTRY

Pterostilbene Suppressed Lipopolysaccharide-Induced Up-Expression of iNOS and COX-2 in Murine Macrophages

MIN-HSIUNG PAN,*,† YEN-HUI CHANG,† MEI-LING TSAI,† CHING-SHU LAI,† SHENG-YOW HO,‡ VLADIMIR BADMAEV,§ AND CHI-TANG HO||,⊥

Department of Seafood Science, National Kaohsiung Marine University, Kaohsiung 811, Taiwan; Department of Radiation Oncology, Sin-Lau Christian Hospital, and Department of Nursing, Chang-Jung Christian University, Tainan, Taiwan; Sabinsa Corporation, 70 Ethel Road West Unit 6, Piscataway, New Jersey 08854; Department of Food Science, Rutgers University, New Brunswick, New Jersey 08901; and Graduate Institute of Food Science and Technology, National Taiwan University, Taipei 100, Taiwan

Pterostilbene, an active constituent of blueberries, is known to possess anti-inflammatory activity and also to induce apoptosis in various types of cancer cells. Here, we investigated the inhibitory effects of pterostilbene on the induction of NO synthase (NOS) and cyclooxygenase-2 (COX-2) in murine RAW 264.7 cells activated with lipopolysaccharide (LPS). Western blotting and real-time polymerase chain reaction (PCR) analyses demonstrated that pterostilbene significantly blocked the protein and mRNA expression of iNOS and COX-2 in LPS-induced macrophages. Treatment with pterostilbene resulted in the reduction of LPS-induced nuclear translocation of the nuclear factor-κB (NFκB) subunit and the dependent transcriptional activity of NFκB by blocking phosphorylation of inhibitor κB (IκB)α and p65 and subsequent degradation of IκBα. Transient transfection experiments using NFκB reporter constructs indicated that pterostilbene inhibits the transcriptional activity of NFκB in LPS-stimulated mouse macrophages. We found that pterostilbene also inhibited LPS-induced activation of PI3K/Akt, extracellular signal-regulated kinase 1/2 and p38 MAPK. Taken together, these results show that pterostilbene down regulates inflammatory iNOS and COX-2 gene expression in macrophages by inhibiting the activation of NFκB by interfering with the activation of PI3K/Akt/IKK and MAPK. These results have an important implication for using pterostilbene toward the development of an effective anti-inflammatory agent.

KEYWORDS: Pterostilbene; inducible NO synthesis (iNOS); NFκB; RAW 264.7 monocyte/macrophages; lipopolysaccharide (LPS); mitogen-activated protein (MAPK); phosphatidylinositol 3-kinase (PI3K); cyclooxygenase-2 (COX-2)

INTRODUCTION

Pterostilbene (*trans*-3,5-dimethoxy-4′-hydroxystilbene), a dimethylether analogue of resveratrol, was found to be as effective as resveratrol in preventing carcinogen-induced preneoplastic lesions in a mouse mammary culture model and inhibiting metastatic growth of melanoma cells to the liver (*1, 2*). Pterostilbene has been demonstrated to have a cancer chemopreventive activity similar to that of resveratrol, and it is cytotoxic to a number of cancer cell lines (*3*). Pterostilbene, isolated from *Vaccinium* barriers, together with resveratrol, suppressed aberrant crypt foci formation in the azoxymethane-induced colon carcinogenesis in rats (*4, 5*). A recent report has shown that pterostilbene exhibited anticancer, anti-inflammatory, antioxidant, and analgesic activity (*6*), but the molecular mechanisms remained to be clarified. The present study has been aimed to investigate the effects of pterostilbene on LPS-induced iNOS and COX-2 expression in mouse. Therefore, we intended to examine the molecular mechanisms of pterostilbene in murine macrophages and to explore underlying molecular mechanisms.

Lipopolysaccharide (LPS), a component of the cell walls of Gram-negative bacteria, induces the activation of monocytes and macrophages and involves the production of proinflammatory cytokines (*7*). Nitric oxide (NO) is produced endogenously by a family of nitric oxide synthases (NOSs) with a wide range of physiological and pathophysiological actions (*8, 9*). NOS enzymes are classified into two groups. One group, cNOS, is

* To whom correspondence should be addressed. Phone: (886)-7-361-7141. Fax: (886)-7-361-1261. E-mail: mhpan@mail.nkmu.edu.tw.
† National Kaohsiung Marine University.
‡ Sin-Lau Christian Hospital and Chang-Jung Christian University.
§ Sabinsa Corporation.
|| Rutgers University.
⊥ National Taiwan University.

10.1021/jf800820y CCC: $40.75
Published on Web 07/26/2008

constitutively present in several cell types (e.g., neurons and endothelial cells) (*10*). The other group, the inducible form (iNOS), which is expressed in various cell types, including macrophages, is induced in response to proinflammatory cytokines and bacterial lipopolysaccharide (LPS) (*11, 12*). Increased NOS expression and/or activity has been reported in human gynecological (*13*), breast (*14*), and central nervous system (*15*) tumors. The mechanism of the signal transduction cascade involved in the induction of iNOS in response to LPS and cytokines is an active area of investigation (*16*).

Cyclooxygenase-2 (COX-2) is an inducible enzyme catalyzing the conversion of arachidonic acid to prostaglandins. Recent studies have suggested that increased levels of prostaglandins and cyclooxygenase activity may play important roles in multiple epithelial cancers such as colon carcinoma (*17, 18*). COX-2-derived bioactive lipids, including prostaglandin E_2, are potent inflammatory mediators that promote tumor growth and metastasis by stimulating cell proliferation, invasion, and angiogenesis (*19*). Therefore, high levels of prostaglandins may promote the development of malignancy (*20*).

Previous reports have shown a potential role for tyrosine kinase in LPS promoters that contain 24 transcriptional factor binding sites, including those for the NFκB family, which appear to be essential for the enhanced *iNOS* and *COX-2* gene expression seen in macrophages exposed to LPS (*21, 22*). The p65 NFκB also seems to be responsible for inducing iNOS in astrocytes (*23*). Activation of NFκB by LPS is induced by a cascade of events leading to the activation of inhibitor κB (IκB) kinases (IKKs), which in turn phosphorylates IκB and leads to the degradation of NFκB and its translocation to the nucleus (*24*). In this pathway, NFκB transcriptional activity is independent of IκBα degradation and is regulated by phosphorylation of NFκB. Phosphorylation at Ser 536 on the p65 subunits is mediated by IKK during LPS stimulation (*25*). Ser 536 phosphorylation is responsible for the recruitment of coactivators as p300, promoting the transcriptional activation of NFκB and subsequent production of inflammatory cytokines (*26*). These IKKs can be activated through phosphorylation by upstream kinases, including NFκB-inducing kinase, mitogen-activate protein kinase, and protein kinase C (*27, 28*). In addition, many studies imply cytokine in the induction of transcription activity of NFκB through extracellular signal-regulated 1/2 (ERK)1/2 (p42/44), p38 MAPK, and PI3K/AKT pathways (*29–32*). Importantly, NO has been shown to be involved in regulating cycoloxygenase-2 (COX-2), which plays a pivotal role in colon tumorigenesis (*33*). Collectively, suppression of enzyme induction and the activities of iNOS/COX-2 is an important approach to preventing carcinogenesis in several organs, including the stomach and colon (*34*). The recent emphasis on the role of NO in pathological conditions such as atherosclerosis including hypercholesterolaemia, hypertension, diabetes, smoking, and cardiovascular disease has led to discovery of new therapeutic agents. Here, we found that pterostilbene was able to protect against LPS-induced inflammation by blocking the activation of NFκB, p44/42 MAPK, and PI3K/Akt, thereby inhibiting the iNOS and COX-2 expression.

MATERIALS AND METHODS

Reagents. Lipopolysaccharide (LPS) (*Escherichia coli* 0127:E8), sufanilamide, naphthylethylenediamine dihydrochloride, and dithiothreitol (DTT) were purchased from Sigma Chemical Co. (St. Louis, MO). The sample of pterostilbene used in the studies was isolated from *Pterocarpus marsupium* (*35*). Pterostilbene was synthesized according to the method reported by Pettit et al. (*36*). The purity of pterostilbene was determined by HPLC as higher than 99.2%.

Cell Culture. RAW 264.7 cells, derived from murine macrophages, were obtained from the American Type Culture Collection (Rockville, MD). RAW 264.7 cells were cultured in Roswell Park Memorial Institute (RPMI) 1640 media (without phenol red) supplemented with 10% endotoxin-free, heat-inactivated fetal calf serum (GIBCO, Grand Island, NY), 100 units/mL penicillin, and 100 μg/mL streptomycin. When the cells reached a density of $2-3 \times 10^6$ cells/mL, they were activated by incubation in medium containing *E. coli* LPS (100 ng/mL). Various concentrations of test compounds dissolved in dimethylsulfoxide were added together with LPS. Cells were treated with 0.05% DMSO as vehicle control.

Determination of Prostaglandin E_2 (PGE_2). The culture medium of control and treated cells was collected, centrifuged, and stored at -70 °C until tested. The level of PGE_2 released into the culture medium was quantified using a specific enzyme immunoassay (EIA) according to the manufacturer's instructions (Amersham, Arlington Heights, IL) (*37*).

Nitrite Assay. The nitrite concentration in the culture medium was measured as an indicator of NO production, according to the Griess reaction (*38*). A portion of each supernatant (100 μL) was mixed with the same volume of Griess reagent (1% sulfanilamide in 5% phosphoric acid and 0.1% naphthylethylenediamine dihydrochloride in water). Absorbance of the mixture at 550 nm was measured with an enzyme-linked immunosorbent assay plate reader (Dynatech MR-7000; Dynatech Laboratories, Chantilly, VA).

Cytotoxicity Assay. The RAW 264.7 cells were cultivated at a density of 2×10^5 cells in a six-well plate. The pterostilbene studied was added to the medium 18 h after inoculation. The cells were harvested after 18 h. Viability was determined by trypan blue exclusion and microscopy examination.

Western Blotting. Afterward, the stimulated murine macrophage cell line RAW 264.7 cells were washed with PBS and lysed in an ice-cold RIPA buffer (Tris-HCl, pH 7.2, 25 mM; 0.1% SDS; 1% Triton X-100; 1% sodium deoxycholate; 0.15 M NaCl; 1 mM EDTA) containing 1 mM phenyl methyl sulfonyl fluoride (PMSF), 10 μg/mL aprotinin, 1 mM sodium orthovanadate, and 5 μg/mL leupeptin. Protein concentrations were determined using the BCA method (Pierce, Rockford, IL). The samples (50 μg of protein) were mixed with 5-fold sample buffer containing 0.3 M Tris-HCl (pH 6.8), 25% 2-mercaptoethanol, 12% sodium dodecyl sulfate (SDS), 25 mM EDTA, 20% glycerol, and 0.1% bromophenol blue. The mixtures were boiled at 100 °C for 5 min, prerun on a stacking gel, and then resolved by 12% SDS-polyacrylamide minigels at a constant current of 20 mA. For electrophoresis, proteins on the gel were electro-transferred onto a 45 μm immobile membrane (PVDF; Millipore Corp., Bedford, MA) with a transfer buffer composed of 25 mM Tris-HCl (pH 8.9), 192 mM glycine, and 20% methanol, as described previously (*39*). The membrane was then incubated with the primary antibody of COX-2 or iNOS (Transduction Laboratories, Lexington, KY) and cytosolic fraction (for IκBα, p65). The membrane was blocked overnight at room temperature with blocking solution (20 mM Tris-HCl pH 7.4, 125 mM NaCl, 0.2% Tween 20, 1% bovine serum albumin, and 0.1% sodium azide), antiphospho (Ser 32)-specific IκBα (New England Biolabs, Ipwich, MA), or anti-β-Actin monoclonal antibodies (Oncogene Science Inc., Uniondale, NJ) at room temperature for 1 h. The antiphospho-Akt (Ser473), antiphospho-p65 (Ser536), antiphospho-p38 (Thr180/Tyr182), antiphospho-JNK, antiphospho-ERK1/2 (Thr202/Tyr204), ERK, JNK, p38, and Akt antibodies obtained from Cell Signaling Technology (Beverly, MA) were used to determine the level of phosphorylated proteins. The membranes were subsequently probed with antimouse or antirabbit IgG antibody conjugated to horseradish peroxidase (Transduction Laboratories, Lexington, KY) and visualized using enhanced chemiluminescence (ECL, Amersham). The densities of the bands were quantitated with a computer densitometer (AlphaImager 2200 System). All the membranes were stripped and reprobed for β-Actin (Sigma Chemical Co., St. Louis, MO) as loading control.

Quantitative Real-Time Reverse-Transcription Polymerase Chain Reaction. Total RNA of cells was extracted using TRIZOL reagent according to the supplier's protocol. The concentration of RNA content was determined by measuring the UV absorbance at 260 and 280 nm, and the RNA was stored at -70 °C until real-time PCR analysis. A

Table 1. PCR Primers and TaqMan Probes Used in the Experiment

genebank accession nos.	name	sequence	probe (no.)
NM_011198.2	*Mus musculus* prostaglandin-endoperoxide synthase 2 (COX-2)	forward: gggagtctggaacattgtgaa reverse: gcacgttgattgtaggtggactgt	4
AY090567.1	*Mus musculus* strain ICR inducible nitric oxide synthase (iNOS)	forward: accctaagagtcaccaaaatgg reverse: ccagggattctggaacattct	17
M12481.1	mouse cytoplasmic β-Actin mRNA (β-Actin)	forward: ccaaccgtgaaaagatgacc reverse: accagaggcatacagggaca	64

total of 2 μg of RNA was transcribed into cDNA using SuperScript II RNase H- reverse transcriptase (Invitrogen, Renfrewshire, U.K.) in a final volume of 20 μL. RT reactions were performed at 42 °C, 50 min, and 99 °C, 5 min, in a Gene Cycler thermal cycler (Bio-Rad). Negative controls were simultaneously performed by including all of the components except RT.

In the real-time PCR analysis, specific primers and a fluorogenic probes were designed to target the conserved regions of various genes using the Lightcycler (LC) probe design software (Roche), according to the manufacture's guidelines for the design of PCR primers and TaqMan probes. The PCR primers and TaqMan probes used in this experiment are listed in **Table 1**.

All TaqMan PCR primers were located in two different exons of each gene to avoid amplification of any contaminating genomic DNA. All PCR reactions were performed using the LightCycler System (Roche Diagnostics, Switzerland) in a total volume of 20 μL containing 1× Taq polymerase buffer, 5 mmol/L $MgCl_2$, 200 μmol/L deoxynucleotides, 300 nmol/L each primer, 150 nmol/L probe, 1 U Taq polymerase, and 20 ng of cDNA. Water instead of cDNA template was used for the negative controls. The gene amplification was done in duplicate for each sample. The thermal cycling conditions are 5 min at 94 °C, followed by 45 cycles, in which each cycle was at 94 °C for 15 s and at 60 °C for 1 min. The relative expression level of the gene in the samples was calculated with the LightCycler software and normalized with housekeeping control (β-Actin).

Transient Transfection and Luciferase Assay. The luciferase assay was performed as described by George et al. (*40*) with some modifications. RAW 264.7 cells were seeded in a 60 mm dish. When the cells reached confluence, the medium was replaced with serum-free Opti-MEM (Gibco). The cells were then transfected with the pNFκB-Luc plasmid reporter gene (Stratagene, Jalla, CA) using LipofectAMINE reagent (Gibo, NRL, Life Technologies, Inc.). After 24 h of incubation, the medium was replaced with complete medium. After another 24 h, the cells were trypsinized and equal numbers of cells were plated in 12-well tissue culture plates for 18 h. The cells were then incubated with 100 ng/mL LPS and pterostilbene for 3 h. Each well was then washed twice with cold PBS and harvested in 150 μL of lysis buffer (0.5 M HEPES pH 7.8, 1% Triton N-101, 1 mM $CaCl_2$, and 1 mM $MgCl_2$). Luciferase activity was assayed by means of the LucLite luciferase reporter gene kit (Packard BioScience Company, Meriden, CT), with 100 μL of cell lysate used in each assay. Luminescence was measured on a top counter microplate scintillation and luminescence counter (Packard 9912 V) in single photon counting mode for 0.1 min/well, following a 5 min adaptation in the dark. Luciferase activities were determined and normalized to protein concentrations.

Statistical Analysis. Data are presented as means ± SE for the indicated number of independently performed experiments. One way Student's *t*-test was used to assess the statistical significance between the LPS- and pterostilbene plus LPS-treated cells. A P value < 0.05 was considered statistically significant.

RESULTS

Inhibition of LPS-Induced Nitrite and PGE_2 Production Pterostilbene in RAW 264.7 Macrophages. To investigate the anti-inflammatory effect of pterostilbene (**Figure 1A**), we tested their effect on nitrite and prostaglandin production in LPS-activated macrophages. Pterostilbene at 30 μM did not interfere with the reaction between nitrite and Griess reagents (data not shown). As shown in **Figure 2**, pterostilbene inhibited nitrite production by >50% at 10 μM. Pterostilbene, at a concentration range 1−30 μM, markedly and concentration-dependently suppressed nitrite production. After treatment with LPS for 24 h, the medium concentration of PGE_2 had elevated significantly to 6.4 ng/mL. This increase was markedly inhibited by different concentrations of pterostilbene (**Figure 3**). Inhibition of nitrite and PGE_2 production was not toxic, as determined by the trypan blue exclusion assay (**Figure 1B**).

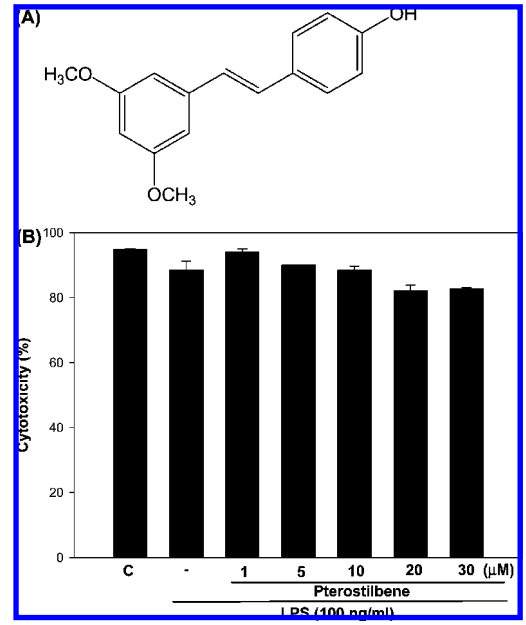

Figure 1. (**A**) Chemical structure of pterostilbene. (**B**) Cytotoxic effects of pterostilbene in RAW 264.7 cells. Cytotoxicity was estimated by trypan blue exclusion using a hemocytometer chamber. The values are expressed as means ± standard error of triplicate tests.

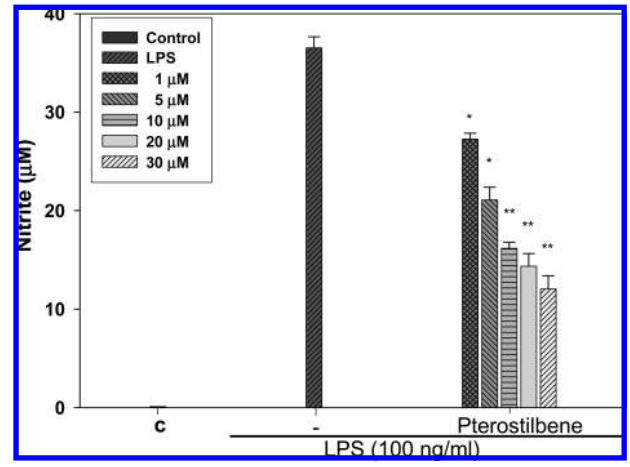

Figure 2. Effects of pterostilbene on LPS-induced nitrite production in RAW 264.7 macrophage. The cells were treated with 100 ng/mL of LPS only or with different concentrations of pterostilbene for 24 h. At the end of incubation time, 100 μL of the culture medium was collected for nitrite assay. The values are expressed as means ± standard error of triplicate tests. *$P < 0.05$ and **$P < 0.01$, indicating statistically significant differences from the LPS-treated group.

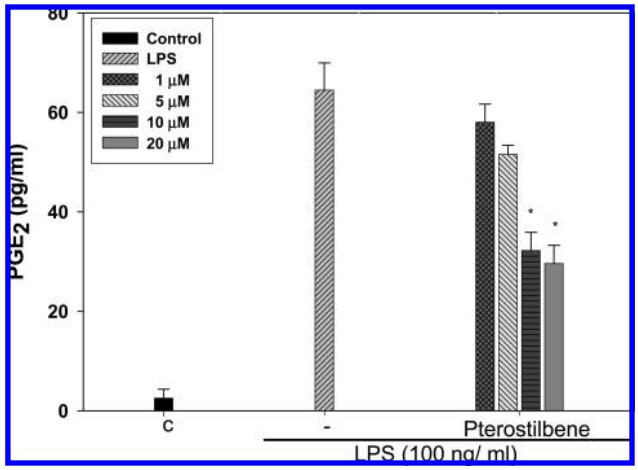

Figure 3. Effects of pterostilbene on LPS-induced PGE_2 production in RAW 264.7 macrophage. The cells were treated with 100 ng/mL of LPS only or with different concentrations and pterostilbene (1 and 20 μM) for 24 h. At the end of incubation time, 100 μL of the culture medium was collected for the PGE_2 assay. The values are expressed as means ± standard error of triplicate tests. *P < 0.05 and **P < 0.01, indicating statistically significant differences from the LPS-treated group.

Pterostilbene Inhibition of LPS-Induced iNOS and COX Gene Expression. We next investigated whether pterostilbene might affect levels of iNOS and COX-2 proteins. As shown in **Figure 4**A, pterostilbene strongly and concentration-dependently suppressed the protein levels of both iNOS and COX-2. These data suggest that translational events are involved in pterostilbene's inhibition of LPS-induced expression of iNOS and COX-2. Changes in the amounts of iNOS and COX-2 enzymes could reflect altered protein synthesis or degradation. Real-time PCR analysis was done to investigate whether pterostilbene suppressed LPS-mediated induction of iNOS and COX-2 via a pretranslational mechanism. From the result of this experiment, we have found that there is a statistically significant (P < 0.01) suppression of *iNOS* and *COX-2* (*β-Actin* as control gene) gene expression in a dose-dependent manner in LPS-activated macrophages (**Figure 4B, C**). These data suggest that pterostilbene may inhibit the expression of iNOS and COX-2 at the transcription levels. The inhibitory effect of pterostilbene on iNOS and COX-2 activities in LPS-activated macrophages was further studied in detail.

Reduction of Nuclear NFκB Level and NFκB Activation by Pterostilbene Treatment in LPS-Stimulated Macrophages. Because activation of NFκB is critical for induction of both iNOS and COX-2 by LPS or other inflammatory cytokines, we used nuclear accumulation to test whether pterostilbene would perturb the distribution of NFκB subunits. Nucleus and cytosolic extracts were prepared and subjected to immunoblot analysis. As shown in **Figure 5A**, coincubation with LPS plus pterostilbene decreased NFκB proteins in the nucleus. PARP, a nuclear protein, and β-Actin, a cytosolic protein, were used as controls to confirm that there was no contamination during extraction of each fraction. In an additional study, transient transfection with a NFκB-dependent luciferase reporter plasmid was done to confirm whether pterostilbene inhibited NFκB binding activity in LPS-induced macrophages. As shown in **Figure 5B**, pterostilbene inhibited LPS-induced NFκB transcriptional activity in a dose-dependent manner.

Inhibitory Effects of Pterostilbene on LPS-Induced Phosphorylation and Degradation of IκBα. Because the LPS-mediated translocation of NFκB to the nucleus is preceded by the phosphorylation and proteolytic degradation of IκBα, we

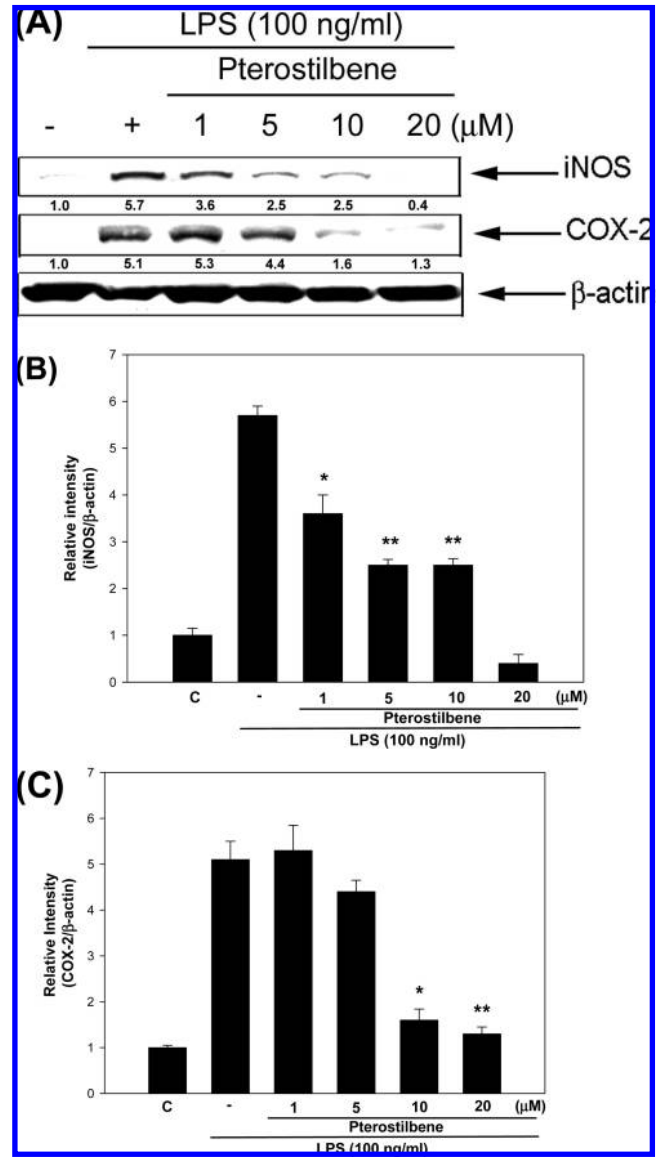

Figure 4. Effects of pterostilbene on LPS-induced iNOS and COX-2 protein expression in RAW 264.7 cells. (**A**) The cells were treated with different concentrations of pterostilbene for 24 h. Equal amounts of total proteins (50 μg) were subjected to 10% SDS-PAGE. The expression of iNOS, COX-2, and β-Actin protein was detected by Western Blot using specific antibodies. This experiment was repeated three times with similar results. (**B**, **C**) Real-time PCR analyses of the expression of iNOS and COX-2 mRNA. Cells were treated with LPS (100 ng/mL) and pterostilbene (1−20 μM) for 5 h; the mRNA expression of *iNOS* and *COX-2* genes was performed using the LighCycler System and TaqMan probe real-time PCR. The values are expressed as means ± standard error of triplicate tests. *P < 0.05 and **P < 0.01, indicating statistically significant differences from the LPS-treated group.

examined the phosphorylated and unphosphorylated protein levels of IκBα by immunoblot analysis. It was found that the treatment with LPS caused the serine-phosphorylation of IκBα protein, as evidenced by the presence of anti-Ser32-phospho-specific IκBα antibody after 15−60 min and the degradation of IκBα after 30 min. Levels of IκBα gradually recovered after 45−60 min. (**Figure 6A**). As shown in **Figure 6B**, treatment with pterostilbene effectively sustained the IκBα protein content. The pattern of inhibition on IκBα phosphorylation by pterostilbene was paralleled to the pattern of inhibition on its degradation. These results suggest that, by blocking the phos-

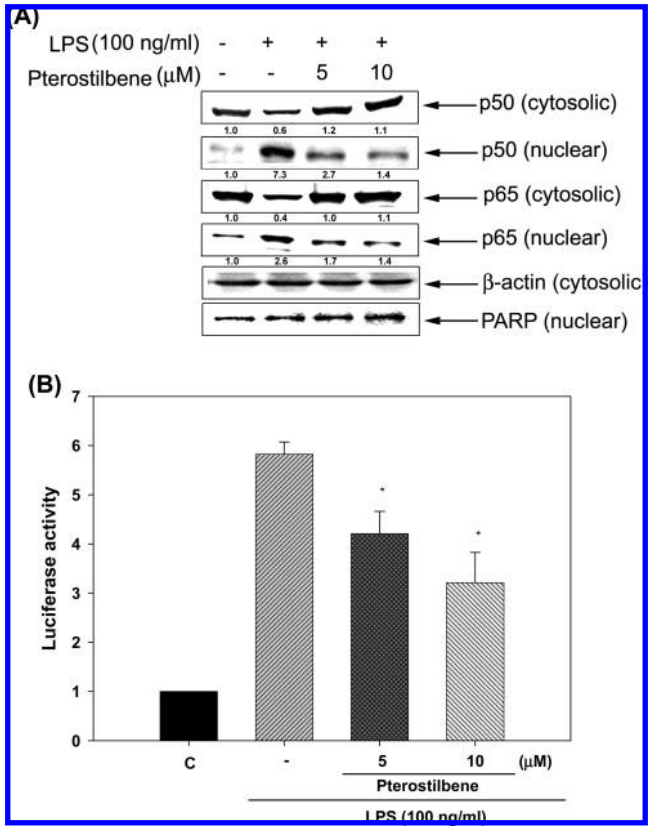

Figure 5. Effects of pterostilbene on LPS-induced p65 and p50 translocation and NFκB activation in RAW264.7 cells. (**A**) Cells were treated with LPS (100 ng/mL) with or without pterostilbene (5 or 10 μM) for 45 min. Then, cytosolic and nuclear fractions were prepared and analyzed by Western Blotting. (**B**) The cells were transiently transfected with 2 μg of pNFκB-Luc reporter gene and then treated with LPS (100 ng/mL) with or without pterostilbene for 12 h. Cells were harvested, and the levels of luciferase activities were determined as described in the Materials and Methods section. Results show the means ± standard error of triplicate tests. *P < 0.05 vs LPS treatment.

phorylation and the degradation of IκBα protein, pterostilbene can inhibit the production of NO and PGE_2 thus preventing the translocation and activation of NFκB in the nucleus (**Figure 5**).

Effects of Pterostilbene on Activation of ERK1/2 (p44/42), p38 MAP kinase, PI3K, and Akt. Because ERK1/2 (p44/42) and p38 MAPK have been shown to be involved in the LPS-mediated induction of iNOS and COX-2 in mouse macrophages (*41, 42*) and cytokine activation of PI3K/Akt pathway leads to the phosphorylation and activation of the NFκB (*43*), we investigated the effects of pterostilbene on the activation of ERK1/2, p38 MAPK, and PI3K/Akt in LPS-stimulated macrophages. Activation of MAPK requires phosphorylation of threonine and tyrosine residues (*44*). When the cells were cotreated with both pterostilbene and LPS for 30 min, pterostilbene was found to attenuate the LPS-stimulated activation of ERK1/2 and p38 MAPK (**Figure 7A**, **B**) but not affect LPS's activation of JNK (**Figure 7C**).We used immunoblot analysis with anti-p85 antibody to investigate whether PI3K pathway was involved in the pterostilbene's inhibition of LPS-induced RAW 264.7 macrophages. We detected PI3K activity. The LPS-stimulated activation of PI3K was attenuated by pterostilbene (**Figure 7C**). To further evaluate the involvement of Akt, a downstream target of PI3K, in LPS-induced responses, we used immunoblot analysis with antiphospho-Akt antibody to examine Akt activity in macrophage cells. When the cells were cotreated

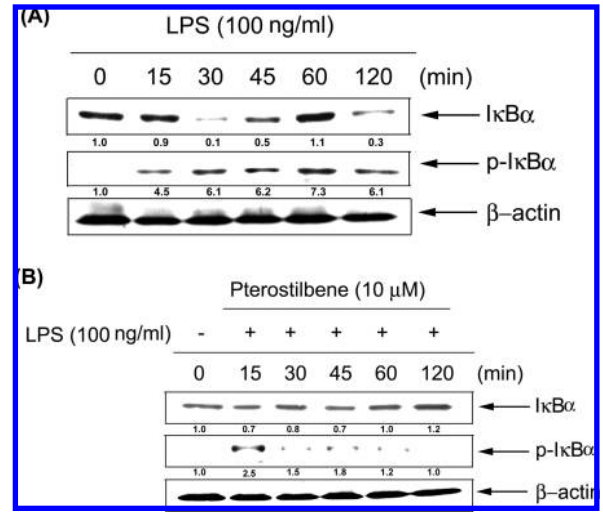

Figure 6. Effects of pterostilbene on LPS-induced phosphorylation and degradation of IκBα. (**A**) RAW 264.7 cells were treated with LPS (100 ng/mL) for different times. Total cellular lysates were prepared for Western Blot analysis. (**B**) Cells were treated with LPS (100 ng/mL) and pterostilbene (10 μM) for different times, and the cellular lysates were prepared and analyzed for content of IκBα, *P*-IκBα, and β-Actin by Western Blot. These experiments were repeated three times with similar results.

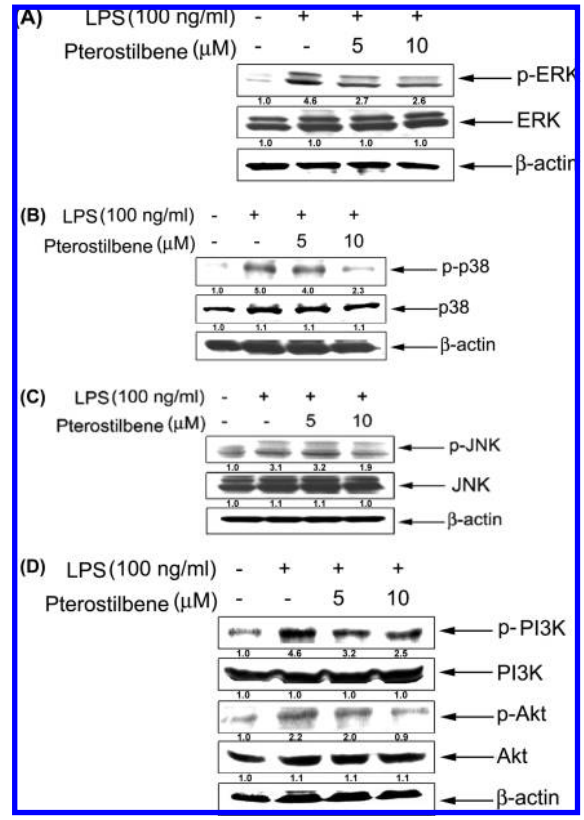

Figure 7. Inhibition of ERK1/2, p38 MAPK, and PI3K/Akt by pterostilbene in LPS-activated RAW macrophages. RAW 264.7 cells were treated with LPS (100 ng/mL) with or without pterostilbene (5 or 10 μM) for 30 min. Cells extracts were then prepared and analyzed for (**A**) p44/42 and *P*-p44/42, (**B**) p38 and *P*-p38, (**C**) *P*-JNK and JNK, or (**D**) *P*-PI3K and *P*-Akt by Western Blot. These experiments were repeated three times with similar results.

with pterostilbene and LPS for 30 min, the LPS-stimulated activation of Akt was attenuated by pterostilbene in a dose-dependent manner (**Figure 7C**). These results of our immunoblot

analyses suggest that pterostilbene's inhibition of iNOS and COX-2 expression might block LPS-induced NFκB activation by inhibiting the ERK1/2, p38, and PI3K/Akt/IKK pathway, which interrupts the degradation of IκBα.

DISCUSSION

Epidemiological studies have linked the consumption of fruits and vegetables to reduced risk of several types of human cancer (*45*). Laboratory animal studies have provided evidence that pterostilbene significantly suppressed azoxymethane-induced formation of ACF and multiple clusters of aberrant crypts and inhibited AOM-induced iNOS expression (*46*). Recent study indicated that rats were dosed i.v. with 20 mg/kg pterostilbene and found that a pterostilbene glucuronidated metabolite was detected in both serum and urine. The in vitro metabolism in rat liver microsomes furthermore suggests phase II metabolism of pterostilbene (*47*). Moreover, pterostilbene has been reported to exhibit many biological effects including anti-inflammatory activity (*6*), but their anti-inflammatory mechanism is still not clear. In the present study, for the first time, we have examined the effects and mechanisms of pterostilbene on LPS-induced expression of iNOS and COX-2. In this study, we found that pterostilbene was a strong inhibitor of iNOS and COX-2 expression in LPS-activated macrophages (**Figure 4**).

Because there is a causal relationship between inflammation and cancer, iNOS and COX-2 are considered potential molecular targets for chemoprevention (*48, 49*). Our present results suggest that pterostilbene's inhibition of the ERK1/2, p38 MAPK, and PI3K/Akt signaling pathway may partially explain how it reduces the induction of the iNOS and COX-2 proteins. In contrast, pterostilbene did not affect the JNK signaling cascade elicited by LPS in macrophages. The possible mechanism is that pterostilbene down regulates inflammatory *iNOS* and *COX-2* gene expression in macrophages by inhibiting the activation NFκB by interfering with the activation of PI3K/Akt and MAPK.

Activation of NFκB is necessary for LPS induction of the iNOS and COX-2 promoters (*50*). NFκB is composed mainly of two proteins, p50 and p65. In resting cells, the NFκB heterodimer is held in the cytosol through interaction with IκB inhibitory proteins (*51*). With exposure to proinflammatory stimuli, IκB becomes phosphorylated, ubiquitinated, and then degraded. Thus, the liberated NFκB dimers are translocated to the nucleus, where the transcription of the target gene is induced. Our results show that pterostilbene reduces iNOS and COX-2 expression by blocking transcription of their genes, a conclusion supported by the observation that it reduced the steady state of iNOS and COX-2 mRNA levels, and promoter activity (as assessed by leuciferase activity assay). Phosphorylation plays an important role in activating protein tyrosine kinase. Many signaling pathways, including PI3K/Akt and mitogen-activated protein kinase, have been proposed to respond to LPS stimulation (*52*). PI3K activation leads to phosphorylation of phosphatidylinositides, which then activate the downstream main target, Akt, which appears to play various important roles in regulating cellular growth, differentiation, adhesion, and the inflammatory reaction (*53*). Activation of PI3K/Akt plays an important role in the expression of iNOS and COX-2 in vascular smooth muscle cells, peritoneal macrophages, and mesangial cells (*54, 55*). Our findings showed the PI3K/Akt pathway to be involved in pterostilbene's inhibition of expression of NFκB-related iNOS and COX-2. In this study, we found that incubation of RAW 264.7 cells with LPS brought about the activation of p38 and ERK1/2. We also found that cotreatment of pterostilbene only blocked the activation of ERK1/2 and p38MAPK. These results suggest that pterostilbene suppresses LPS-induced NFκB translocation by inhibiting the activation of MAPK and subsequently decreasing the protein levels of iNOS and COX-2.

On the basis of our above findings, we are proposing pterostilbene to be a potential and novel chemopreventive agent and may be used in the future to treat inflammation-associated tumorigenesis. The possible relationship between the structural properties of pterostilbene and their anti-inflammatory and anticarcinogenic activities deserves further investigation.

ABBREVIATIONS USED

iNOS, inducible nitric oxide synthase; LPS, lipopolysaccharide; NO, nitric oxide; COX-2, cycoloxygenase-2; PGE_2, prostaglandin E_2; IκB, inhibitor κB; NFκB, nuclear factor κB; MAPK, mitogen-activated protein kinase.

LITERATURE CITED

(1) Ferrer, P.; Asensi, M.; Segarra, R.; Ortega, A.; Benlloch, M.; Obrador, E.; Varea, M. T.; Asensio, G.; Jorda, L.; Estrela, J. M. Association between pterostilbene and quercetin inhibits metastatic activity of B16 melanoma. *Neoplasia* **2005**, *7* (1), 37–47.

(2) Rimando, A. M.; Cuendet, M.; Desmarchelier, C.; Mehta, R. G.; Pezzuto, J. M.; Duke, S. O. Cancer chemopreventive and antioxidant activities of pterostilbene, a naturally occurring analogue of resveratrol. *J. Agric. Food Chem.* **2002**, *50* (12), 3453–3457.

(3) Rimando, A. M.; Cuendet, M.; Desmarchelier, C.; Mehta, R. G.; Pezzuto, J. M.; Duke, S. O. Cancer chemopreventive and antioxidant activities of pterostilbene, a naturally occurring analogue of resveratrol. *J. Agric. Food Chem.* **2002**, *50* (12), 3453–3457.

(4) Suh, N.; Paul, S.; Hao, X.; Simi, B.; Xiao, H.; Rimando, A. M.; Reddy, B. S. Pterostilbene, an active constituent of blueberries, suppresses aberrant crypt foci formation in the azoxymethane-induced colon carcinogenesis model in rats. *Clin. Cancer Res.* **2007**, *13* (1), 350–355.

(5) Rimando, A. M.; Kalt, W.; Magee, J. B.; Dewey, J.; Ballington, J. R. Resveratrol, pterostilbene, and piceatannol in vaccinium berries. *J. Agric. Food Chem.* **2004**, *52* (15), 4713–4719.

(6) Remsberg, C. M.; Yanez, J. A.; Ohgami, Y.; Vega-Villa, K. R.; Rimando, A. M.; Davies, N. M. Pharmacometrics of pterostilbene: preclinical pharmacokinetics and metabolism, anticancer, antiinflammatory, antioxidant and analgesic activity. *Phytother. Res.* **2008**, *22* (2), 169–179.

(7) Nicholas, C.; Batra, S.; Vargo, M. A.; Voss, O. H.; Gavrilin, M. A.; Wewers, M. D.; Guttridge, D. C.; Grotewold, E.; Doseff, A. I. Apigenin blocks lipopolysaccharide-induced lethality in vivo and proinflammatory cytokines expression by inactivating NF-κB through the suppression of p65 phosphorylation. *J. Immunol.* **2007**, *179* (10), 7121–7127.

(8) Moncada, S.; Palmer, R. M.; Higgs, E. A. Nitric oxide: physiology, pathophysiology, and pharmacology. *Pharmacol. Rev.* **1991**, *43* (2), 109–142.

(9) Nathan, C.; Xie, Q. W. Nitric oxide synthases: roles, tolls, and controls. *Cell* **1994**, *78* (6), 915–918.

(10) Liu, R. H.; Hotchkiss, J. H. Potential genotoxicity of chronically elevated nitric oxide: a review. *Mutat. Res.* **1995**, *339* (2), 73–89.

(11) Rockey, D. C.; Chung, J. J.; McKee, C. M.; Noble, P. W. Stimulation of inducible nitric oxide synthase in rat liver by hyaluronan fragments. *Hepatology* **1998**, *27* (1), 86–92.

(12) Geller, D. A.; Lowenstein, C. J.; Shapiro, R. A.; Nussler, A. K.; Di, S. M.; Wang, S. C.; Nakayama, D. K.; Simmons, R. L.; Snyder, S. H.; Billiar, T. R. Molecular cloning and expression of inducible nitric oxide synthase from human hepatocytes. *Proc. Natl. Acad. Sci. U. S. A.* **1993**, *90* (8), 3491–3495.

(13) Thomsen, L. L.; Lawton, F. G.; Knowles, R. G.; Beesley, J. E.; Riveros-Moreno, V.; Moncada, S. Nitric oxide synthase activity in human gynecological cancer. *Cancer Res.* **1994**, *54* (5), 1352–1354.

(14) Thomsen, L. L.; Miles, D. W.; Happerfield, L.; Bobrow, L. G.; Knowles, R. G.; Moncada, S. Nitric oxide synthase activity in human breast cancer. *Br. J. Cancer* **1995**, *72* (1), 41–44.

(15) Cobbs, C. S.; Brenman, J. E.; Aldape, K. D.; Bredt, D. S.; Israel, M. A. Expression of nitric oxide synthase in human central nervous system tumors. *Cancer Res.* **1995**, *55* (4), 727–730.

(16) Liu, Q. P.; Fruit, K.; Ward, J.; Correll, P. H. Negative regulation of macrophage activation in response to IFN-γ and lipopolysaccharide by the STK/RON receptor tyrosine kinase. *J. Immunol.* **1999**, *163* (12), 6606–6613.

(17) Levy, G. N. Prostaglandin H synthases, nonsteroidal anti-inflammatory drugs, and colon cancer. *FASEB J.* **1997**, *11* (4), 234–247.

(18) Dubois, R. N.; Abramson, S. B.; Crofford, L.; Gupta, R. A.; Simon, L. S.; Van De Putte, L. B.; Lipsky, P. E. Cyclooxygenase in biology and disease. *FASEB J.* **1998**, *12* (12), 1063–1073.

(19) Mann, J. R.; Backlund, M. G.; DuBois, R. N. Mechanisms of disease: Inflammatory mediators and cancer prevention. *Nat. Clin. Pract. Oncol.* **2005**, *2* (4), 202–210.

(20) Yoshimura, R.; Matsuyama, M.; Tsuchida, K.; Takemoto, Y.; Nakatani, T. Relationship between cyclooxygenase (COX)-2 and malignant tumors. *Nippon Rinsho* **2005**, *63* (10), 1839–1848.

(21) Xie, Q. W.; Kashiwabara, Y.; Nathan, C. Role of transcription factor NF-κB/Rel in induction of nitric oxide synthase. *J. Biol. Chem.* **1994**, *269* (7), 4705–4708.

(22) Pan, M. H.; Lai, C. S.; Wang, Y. J.; Ho, C. T. Acacetin suppressed LPS-induced up-expression of iNOS and COX-2 in murine macrophages and TPA-induced tumor promotion in mice. *Biochem. Pharmacol.* **2006**, *72* (10), 1293–1303.

(23) Feinstein, D. L.; Galea, E.; Aquino, D. A.; Li, G. C.; Xu, H.; Reis, D. J. Heat shock protein 70 suppresses astroglial-inducible nitric-oxide synthase expression by decreasing NFκB activation. *J. Biol. Chem.* **1996**, *271* (30), 17724–17732.

(24) Griscavage, J. M.; Wilk, S.; Ignarro, L. J. Inhibitors of the proteasome pathway interfere with induction of nitric oxide synthase in macrophages by blocking activation of transcription factor NF-κB. *Proc. Natl. Acad. Sci. U. S. A.* **1996**, *93* (8), 3308–3312.

(25) Yang, F.; Tang, E.; Guan, K.; Wang, C. Y. IKK β plays an essential role in the phosphorylation of RelA/p65 on serine 536 induced by lipopolysaccharide. *J. Immunol.* **2003**, *170* (11), 5630–5635.

(26) Chen, Y.; Vallee, S.; Wu, J.; Vu, D.; Sondek, J.; Ghosh, G. Inhibition of NF-κB activity by IκBβ in association with κB-Ras. *Mol. Cell Biol.* **2004**, *24* (7), 3048–3056.

(27) Chio, C. C.; Chang, Y. H.; Hsu, Y. W.; Chi, K. H.; Lin, W. W. PKA-dependent activation of PKC, p38 MAPK and IKK in macrophage: implication in the induction of inducible nitric oxide synthase and interleukin-6 by dibutyryl cAMP. *Cell Signal.* **2004**, *16* (5), 565–575.

(28) Kim, J. M.; Oh, Y. K.; Lee, J. H.; Im, D. Y.; Kim, Y. J.; Youn, J.; Lee, C. H.; Son, H.; Lee, Y. S.; Park, J. Y.; Choi, I. H. Induction of proinflammatory mediators requires activation of the TRAF, NIK, IKK and NF-κB signal transduction pathway in astrocytes infected with *Escherichia coli*. *Clin. Exp. Immunol.* **2005**, *140* (3), 450–460.

(29) Je, J. H.; Lee, J. Y.; Jung, K. J.; Sung, B.; Go, E. K.; Yu, B. P.; Chung, H. Y. NF-κB activation mechanism of 4-hydroxyhexenal via NIK/IKK and p38 MAPK pathway. *FEBS Lett.* **2004**, *566* (1−3), 183–189.

(30) Chandrasekar, B.; Marelli-Berg, F. M.; Tone, M.; Bysani, S.; Prabhu, S. D.; Murray, D. R. β-adrenergic stimulation induces interleukin-18 expression via β2-AR, PI3K, Akt, IKK, and NF-κB. *Biochem. Biophys. Res. Commun.* **2004**, *319* (2), 304–311.

(31) Bozinovski, S.; Jones, J. E.; Vlahos, R.; Hamilton, J. A.; Anderson, G. P. Granulocyte/macrophage-colony-stimulating factor (GM-CSF) regulates lung innate immunity to lipopolysaccharide through Akt/Erk activation of NFκB and AP-1 in vivo. *J. Biol. Chem.* **2002**, *277* (45), 42808–42814.

(32) Agarwal, A.; Das, K.; Lerner, N.; Sathe, S.; Cicek, M.; Casey, G.; Sizemore, N. The AKT/IκB kinase pathway promotes angiogenic/metastatic gene expression in colorectal cancer by activating nuclear factor-κB and β-catenin. *Oncogene* **2005**, *24* (6), 1021–1031.

(33) Landino, L. M.; Crews, B. C.; Timmons, M. D.; Morrow, J. D.; Marnett, L. J. Peroxynitrite, the coupling product of nitric oxide and superoxide, activates prostaglandin biosynthesis. *Proc. Natl. Acad. Sci. U. S. A.* **1996**, *93* (26), 15069–15074.

(34) Nosho, K.; Yoshida, M.; Yamamoto, H.; Taniguchi, H.; Adachi, Y.; Mikami, M.; Hinoda, Y.; Imai, K. Association of Ets-related transcriptional factor E1AF expression with overexpression of matrix metalloproteinases, COX-2 and iNOS in the early stage of colorectal carcinogenesis. *Carcinogenesis* **2005**, *26* (5), 892–899.

(35) Mathew, J.; Rao, A. V. S. Chemical examination of pterocarpus marsupium. *J. Indian Chem. Soc.* **1984**, *61* (8), 728–729.

(36) Pettit, G. R.; Grealish, M. P.; Jung, M. K.; Hamel, E.; Pettit, R. K.; Chapuis, J. C.; Schmidt, J. M. Antineoplastic agents. 465. Structural modification of resveratrol: sodium resverastatin phosphate. *J. Med. Chem.* **2002**, *45* (12), 2534–2542.

(37) Suh, N.; Honda, T.; Finlay, H. J.; Barchowsky, A.; Williams, C.; Benoit, N. E.; Xie, Q. W.; Nathan, C.; Gribble, G. W.; Sporn, M. B. Novel triterpenoids suppress inducible nitric oxide synthase (iNOS) and inducible cyclooxygenase (COX-2) in mouse macrophages. *Cancer Res.* **1998**, *58* (4), 717–723.

(38) Kim, H.; Lee, H. S.; Chang, K. T.; Ko, T. H.; Baek, K. J.; Kwon, N. S. Chloromethyl ketones block induction of nitric oxide synthase in murine macrophages by preventing activation of nuclear factor-κB. *J. Immunol.* **1995**, *154* (9), 4741–4748.

(39) Pan, M. H.; Lin-Shiau, S. Y.; Ho, C. T.; Lin, J. H.; Lin, J. K. Suppression of lipopolysaccharide-induced nuclear factor-κB activity by theaflavin-3,3′-digallate from black tea and other polyphenols through down-regulation of IκB kinase activity in macrophages. *Biochem. Pharmacol.* **2000**, *59* (4), 357–367.

(40) George, S. E.; Bungay, P. J.; Naylor, L. H. Functional coupling of endogenous serotonin (5-HT1B) and calcitonin (C1a) receptors in CHO cells to a cyclic AMP-responsive luciferase reporter gene. *J. Neurochem.* **1997**, *69* (3), 1278–1285.

(41) Nick, J. A.; Young, S. K.; Brown, K. K.; Avdi, N. J.; Arndt, P. G.; Suratt, B. T.; Janes, M. S.; Henson, P. M.; Worthen, G. S. Role of p38 mitogen-activated protein kinase in a murine model of pulmonary inflammation. *J. Immunol.* **2000**, *164* (4), 2151–2159.

(42) Ho, F. M.; Lai, C. C.; Huang, L. J.; Kuo, T. C.; Chao, C. M.; Lin, W. W. The anti-inflammatory carbazole, LCY-2-CHO, inhibits lipopolysaccharide-induced inflammatory mediator expression through inhibition of the p38 mitogen-activated protein kinase signaling pathway in macrophages. *Br. J. Pharmacol.* **2004**, *141* (6), 1037–1047.

(43) Sizemore, N.; Leung, S.; Stark, G. R. Activation of phosphatidylinositol 3-kinase in response to interleukin-1 leads to phosphorylation and activation of the NF-κB p65/RelA subunit. *Mol. Cell Biol.* **1999**, *19* (7), 4798–4805.

(44) Raingeaud, J.; Gupta, S.; Rogers, J. S.; Dickens, M.; Han, J.; Ulevitch, R. J.; Davis, R. J. Pro-inflammatory cytokines and environmental stress cause p38 mitogen-activated protein kinase activation by dual phosphorylation on tyrosine and threonine. *J. Biol. Chem.* **1995**, *270* (13), 7420–7426.

(45) Surh, Y. J. Cancer chemoprevention with dietary phytochemicals. *Nat. Rev. Cancer* **2003**, *3* (10), 768–780.

(46) Suh, N.; Paul, S.; Hao, X.; Simi, B.; Xiao, H.; Rimando, A. M.; Reddy, B. S. Pterostilbene, an active constituent of blueberries, suppresses aberrant crypt foci formation in the azoxymethane-induced colon carcinogenesis model in rats. *Clin. Cancer Res.* **2007**, *13* (1), 350–355.

(47) Remsberg, C. M.; Yanez, J. A.; Ohgami, Y.; Vega-Villa, K. R.; Rimando, A. M.; Davies, N. M. Pharmacometrics of pterostilbene: preclinical pharmacokinetics and metabolism, anticancer, antiin-

flammatory, antioxidant and analgesic activity. *Phytother. Res.* **2008**, *22* (2), 169–179.
(48) Surh, Y. J. Cancer chemoprevention with dietary phytochemicals. *Nat. Rev. Cancer* **2003**, *3* (10), 768–780.
(49) Chun, K. S.; Cha, H. H.; Shin, J. W.; Na, H. K.; Park, K. K.; Chung, W. Y.; Surh, Y. J. Nitric oxide induces expression of cyclooxygenase-2 in mouse skin through activation of NF-κB. *Carcinogenesis* **2004**, *25* (3), 445–454.
(50) Xie, Q. W.; Kashiwabara, Y.; Nathan, C. Role of transcription factor NF-κB/Rel in induction of nitric oxide synthase. *J. Biol. Chem.* **1994**, *269* (7), 4705–4708.
(51) Baeuerle, P. A.; Henkel, T. Function and activation of NF-κB in the immune system. *Annu. Rev. Immunol.* **1994**, *12*, 141–179.
(52) Chen, C. C.; Wang, J. K. p38 but not p44/42 mitogen-activated protein kinase is required for nitric oxide synthase induction mediated by lipopolysaccharide in RAW 264.7 macrophages. *Mol. Pharmacol.* **1999**, *55* (3), 481–488.
(53) Carpenter, C. L.; Cantley, L. C. Phosphoinositide kinases. *Curr. Opin. Cell Biol.* 1996*8* (2), 153–158.
(54) Hattori, Y.; Hattori, S.; Kasai, K. Lipopolysaccharide activates Akt in vascular smooth muscle cells resulting in induction of inducible nitric oxide synthase through nuclear factor-κB activation. *Eur. J. Pharmacol.* **2003**, *481* (2−3), 153–158.
(55) Sheu, M. L.; Chao, K. F.; Sung, Y. J.; Lin, W. W.; Lin-Shiau, S. Y.; Liu, S. H. Activation of phosphoinositide 3-kinase in response to inflammation and nitric oxide leads to the up-regulation of cyclooxygenase-2 expression and subsequent cell proliferation in mesangial cells. *Cell Signal.* **2005**, *17* (8), 975–984.

Received for review March 15, 2008. Revised manuscript received May 3, 2008. Accepted June 13, 2008. This study was supported by the National Science Council under Grants No. NSC 96-2321-B-022-001 and No. NSC 95-2313-B-022-003-MY3.

JF800820Y